Magazine of Civil Engineering

ISSN 2712-8172

journal homepage: http://engstroy.spbstu.ru/

DOI: 10.18720/MCE.99.12

Flange connections with high-strength bolts with technological heredity of bolts

N. Vatin*[a], R.G. Gubaydulin[b], A. Tingaev[b]

[a] *Peter the Great St. Petersburg Polytechnic University, St. Petersburg, Russia*

[b] *South Ural State University, Chelyabinsk, Russia*

** E-mail: vatin@mail.ru*

Keywords: delayed brittle fracture, finite element method, flanges, high-strength bolts, joints, non-metallic inclusions, steel structures, stiffness, stress-strain state, struct

Abstract. Tubular truss and column members with bolted connections widely used in construction. The object of this research was the flange joint of a truss bottom chord. The flange joint coaxially connects two cold-formed closed welded rectangular hollow section profiles. The flange connects with high-strength bolts of strength class 10.9. The stress-strain state of the joint was numerically and experimentally investigated. Experimental studies were performed on a full-size sample of a flange joint using strain gauges. Numerical calculations were performed at ANSYS. The bilinear isotropic hardening model simulated the metal elements performance of the joint. The “Frictional” model was chosen for the friction forces between the flanges. The microstructure of the bolt material was studied using an optical microscope. The study results showed that the model solution for a flanged provides a uniform distribution of stresses at the junction due to its spatial rigidity. The presence of stiffener ribs provides the absence of the clearance between the flanges and promotes the joint performance of welded units and high-strength bolts. The design of the flange joint using the developed finite element model indicates that the results of numerical and experimental studies are sufficient for practical application. The difference between finite element model calculations and experimental data in the most loaded elements of flange joints does not exceed 10 %. It is proposed for high-strength bolts of strength class 10.9 and higher to introduce regulatory restrictions on the number and size of non-metallic inclusions that affect the delayed brittle fracture of bolts. To improve the performance that bolts, it is proposed to use steel grades with a bainitic or bainitic-martensitic structure, which are formed by microalloying them with molybdenum, vanadium, niobium, titanium, boron and heat treatment.

1. Introduction

Bolted joints have been widely used in steel structures of buildings. One of the most effective of them is bolted-flange connections with high-strength bolts. The advantages of these joints include the simplicity of assembly, the possibility of work in any climatic conditions, high reliability, and the ability to disassemble them without damage to structural elements [1–6]. Bolted joints may be subject to the combined action of axial compression, bending moments and shearing under the combination of dead, live, wind loads or earthquake action.

Flange connections in structures are subject to tension, compression, tensile bending, seismic actions, and vibration loads with the number of cycles of constant loading up to 105 with an asymmetry coefficient of at least 0.8 [4, 7].

The disadvantages of flange connections include high requirements for the accuracy of their manufacture since this type of connections does not have a proper compensating ability. In particular, experience with flange connections indicates that combinations of unfavorable structural and technological deviations, such as non-planarity of matching surfaces, displacement of hole axes, misalignment of nut and bolt bearing surfaces, etc., increase the likelihood of their failure, especially when using bolts of the strength class 10.9 and higher [8–10].

The design of flange connections is a rather complicated task [10, 3, 11]. As a result, the main provisions of the regulatory methods for calculating flange joints are formulated, which establish three types of design models (rigid, semi-rigid and flexible), which differ in the development of fracture mechanism [12, 13].

In the case of using flexible flanges, the destruction of the joint occurs due to the development of significant plastic deformations in the flange. The bearing capacity of the connection in this case is determined by the bearing capacity of the flange itself, while the forces acting in the bolts do not reach their ultimate state. When using semi-rigid flanges, their bending stiffness increases, and the destruction of the joint occurs due to the destruction of the bolts during the partial development of plastic deformations in the flanges. For joints with rigid flanges, the ultimate state is the destruction of a high-strength bolt, while the stress-strain state of the remaining elements of the flange is characterized by the elastic behavior of the material. The flange thickness has a considerable impact on the connection properties, while the bolt edge distance and the flange edge width were found to have a smaller effect [4, 5, 14, 15].

The design rules for calculating flange joints are mainly based on the experimental results of T-shaped joints' models, which have been tested and refined concerning specific types of joints. For example, in the EU countries, flanged joints with double and four-row arrangement of bolts without stiffeners are widely used, which are more technologically advanced and less demanding to manufacture [12], however, they are unbeneficial in terms of strength and stiffness when compared to flange joints with additional stiffening ribs. In particular, flanged joints without stiffeners with a double-row arrangement of bolts can provide only 30...40 % of the profile strength of the connected elements, and with a four-row arrangement can provide 60...70 % of the profile strength [16].

It should be noted that the design rules for flange joints are valid for certain types of structural solutions and for a limited range of flange thicknesses, which does not allow us to use them in the design of flange joints for technically complex and unique structures. In this regard, the most universal tool for determining the stress-strain state of flange joints, considering the combined behavior of its elements (flanges, bolts and welded joints), is the finite element method. The use of the finite element method allows us to avoid using idealized models and standard design models and to examine in more detail the behavior of individual elements of flange joints considering their geometric and physical nonlinearity.

The effectiveness of applying the finite element method to consider the influence of structural factors on the stress-strain state of flange joints is doubtless [17, 18]. At the same time, it should be noted that to ensure the accuracy of the calculation of the stress-strain state of flange joints, it is necessary to use finite element models validated with experimental tests. The absence of such models is one of the main factors restraining the use of the finite element method as a method for calculating flange joints.

The calculation of the stress-strain state of a flange joint is a necessary but not sufficient condition for ensuring its safe behavior, especially for cases in which its ultimate state is the destruction of high-strength bolts. Single-direction high-strength bolts are mostly used in column-beam joints and conventional high-strength bolts are mostly used in flange connections. Experimental results show that two types of the bolt have different failure models [19]. The failure of the single-direction high-strength bolt is due to the pullout of the bolt, which is caused by the extrusion bending deformation of its outer sleeve [19].

In flange joints, conventional high-strength bolts of strength class 10.9 and higher are characterized by an increased tendency to hydrogen embrittlement [20, 8], in which relatively insignificant changes in the structure, properties and stress-strain state of the bolt, if the combination is unfavorable, can initiate the process of delayed brittle fracture.

Delayed brittle fracture of high-strength bolts is one of the most difficult to predict types of ultimate state [21–26], for which no design rules have yet been developed. Therefore, to reduce the risk of its occurrence, the standard [27] recommends using experimental methods for assessing resistance to delayed brittle fracture, which allows building designers to properly choose a material, manufacturing technology, and anticorrosive protection of bolts.

It follows from the review that the connections of steel structures with rigid flanges, stiffening ribs and high-strength bolts have not been adequately studied. In particular, there is no analysis of the influence of the technological heredity of high-strength bolts on the general characteristics of the flange connection. Technological heredity is the transfer to the finished product in the process of manufacturing errors, mechanical and physical and chemical properties of the original billet or properties and errors formed in the billets in individual operations of manufacturing the product [28].

The work aims to develop recommendations for improving the design of flange joints, as well as recommendations for improving the standards for the quality of high-strength bolts with the risk of delayed brittle fracture.

The objectives of the study are:

1. Analysis of the effectiveness of a typical solution of flange joints according to the results of experimental and numerical studies of the stress-strain state.

2. Studies to assess the influence of technological heredity factors on the performance of high-strength bolts, develop proposals for regulatory restrictions on the number and size of non-metallic inclusions that affect delayed brittle fracture of bolts, develop proposals for the selection of steel grades for the manufacture of bolts.

2. Methods

2.1. The investigated flange joints

This paper experimentally investigated the flanged joint of the truss bottom chord. The flanges were connected by high-strength bolts with a diameter of 24 mm, strength class 10.9 (Fig. 1). The section of the bottom truss chord is made of a cold-formed closed welded rectangular hollow section profile 140×140×4 mm of the S345-3 steel grade according to Russian State Standard GOST 30245-2012 “Steel bent closed welded square and rectangular section for building. Specifications”.

The connection flange is made of 30 mm thick sheet steel of the same grade C345-3 steel grade. The S345-3 steel grade is specified by Russian State Standard GOST 27772-2015 “Hot-rolled steel for building steel structures. General specifications”. The properties of S345-3 steel are given in Tables 1, 2.

Table 1. The S345-3 steel grade chemical decomposition.

Steel grade	Mass fraction, %								
	C	Mn	Si	Cr	Ni	Cu	Al	S	P
S345-3	≥ 0.15	1.30–1.70	≥ 0.80	≥ 0.30	≥ 0.30	≥ 0.30	0.015–0.06	≥ 0.025	≥ 0.030

Table 2. The S345-3 steel grade mechanical properties.

Steel grade	Thickness [mm]	Yield strength σ_y [MPa]	Ultimate strength σ_u [MPa]	Elongation A_5 [%]	Impact strength KCV^{-40} [J/cm^2]
S345-3	4-10	≥ 345	≥4 90	≥ 21	≥ 34
	20-40	≥ 305	≥ 460	≥ 21	≥ 34

The connection of the chord (Tag No. 287) with the flange (Tag No. 34) is made by equal-angle fillet welds with a 4 mm leg (Fig. 2). The stiffeners (Tag No. 75) are connected to the chord by equal-angle fillet welds with a 5 mm leg. All welds are made by mechanized welding in a protective gas medium with welding steel wire of the steel grade Sv-08G2S with a diameter of 1.2 mm. The welding steel wire is specified by Russian State Standard GOST 2246-70 ”Welding steel wire. Technical specifications”. The quality of the welds is confirmed by visual, measuring, and ultrasonic testing.

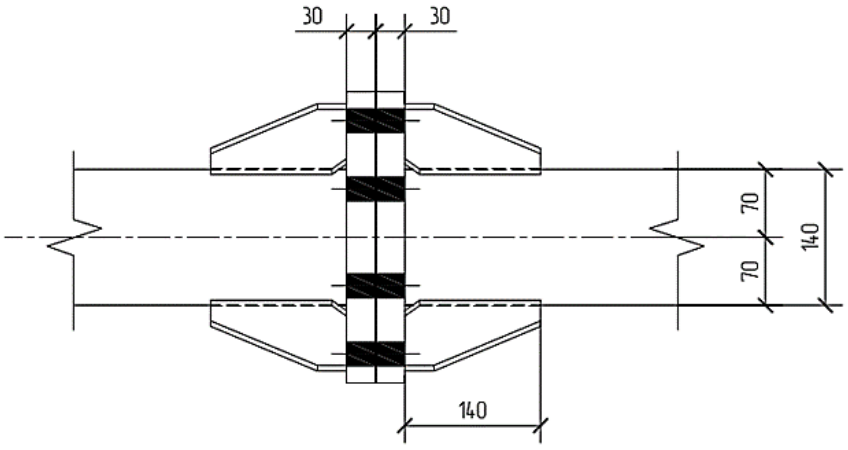

Figure 1. Analyzed joint.

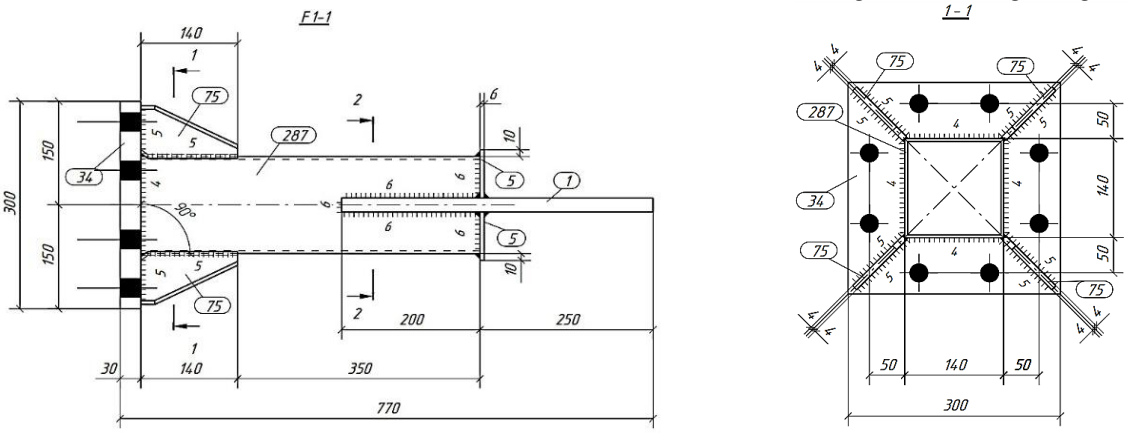

Figure 2. Building block of the full-scale model of the flanged joint of the bottom chord of a truss.

Additional stiffening ribs of this flange connection increase strength and stiffness and reduce its ductility. Such flange connections are in demand for telecommunication towers, masts, frames of high-rise buildings, and other structures. For them, the main requirements are the rotation and displacement angles of individual elements and the structure during operation.

2.2. Experimental investigation

The study was carried out in stages. At the first stage, experimental studies of the stress state of the elements of flange joints by strain gauges were carried out. To measure the relative strains, single-axis foil strain gauge sensors (strain gauges) 2FKP-5x200 with a change base of 5 mm were used. The measuring system received and processed signals of strain gauges. SIIT-3 system is designed to measure up to 100 output signals with a polling speed of at least 20 measurements per second.

The total number of sensors was 75 pcs. The number of sensors at each specific point depended on the orientation of the main stress areas (Fig. 3). If the directions of the main stresses were known, then two strain gauge sensors were installed: one was glued along the direction, and the second was glued across. In all other cases, three sensors were installed according to the rosette-like outline.

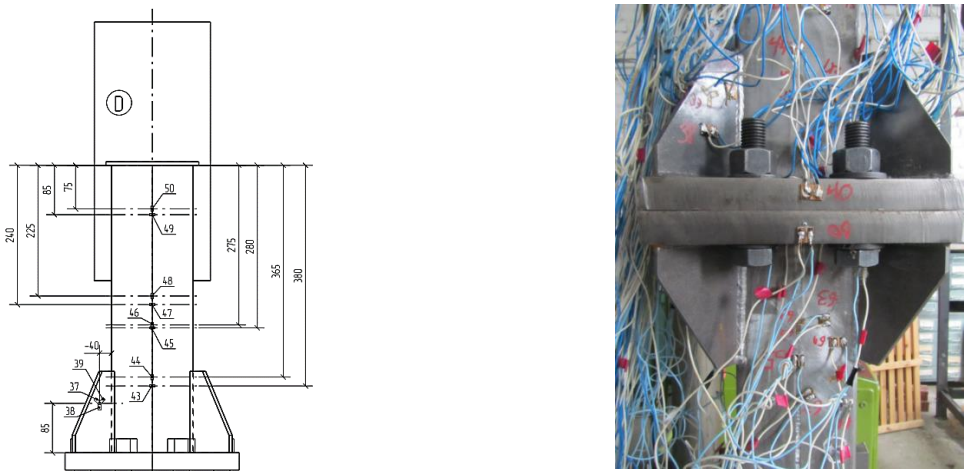

Figure 3. Location of strain gauges on the surface of the flange joint.

The tests were carried out at the South Ural State University (Russia) on the universal testing machine MUP-100 by uniaxial static tension. The load was started from 19.6 kN and applied in increments of 98 kN up to 314 kN. Above 314 kN, the load was applied in increments of 49 kN. The increment values were chosen on the base on FE calculation. At each stage of loading, the readings of the strain gauges were automatically recorded. These readings were then averaged over the results of three measurements.

Before starting the test, the bolts were previously tightened with a force of 267 kN by Tohnichi DBE2100N-S torque wrench.

2.3. . FE models

The Finite element model of the joint was created in ANSYS WorkbenchFE. In the development of the flange connection FE model, the following design features were taken into account [29–32]:

1. The bending moment and the lateral force were not considered in the joint under the applied external load.

2. The external load was uniformly distributed between the bolts.

3. The analytical model cannot be represented in the form of a flat beam system. Therefore, it is necessary to take into account the spatial behavior of the joint in two orthogonal planes.

4. The stress-strain state of the flange and bolts depends on the ratio of the stiffness properties of the connected elements.

To take these features into account, the following assumptions were made:

1. A tensile force is applied along the centerline of the chord.

2. The bolt is modeled by a cylinder. The cross-sectional area of the cylinder in the bolt's thread segment is equal to the net area of the bolt. The cross-sectional area of the cylinder out of the bolt's thread segment is equal to the gross area of the bolt.

3. The contact between the surfaces of the flanges is a tight connection of two surfaces. A shift of one surface along another causes a friction force.

4. The contact of the inner surface of the bolt head and the outer surface of the flange does not interrupt during loading. The friction of one surface relative to another is allowed.

5. To describe the nonlinear properties of the material, a bilinear model with isotropic hardening was chosen. The model establishes the following relationship between load σ and strain ε. The transition from an elastic to a plastic state is determined by the von Mises criterion.

$$\sigma = \begin{cases} E \cdot \varepsilon, & \text{when } \varepsilon \le \sigma_y / E \\ \sigma_y + E_T(\varepsilon - \sigma_y / E), & \text{when } \varepsilon > \sigma_y / E \end{cases},$$

where ε is the current value of the relative deformation of the specimen, σ_y is yield strength, E_T is the tangent module of elasticity, E is Young's modulus. The values of the tangential modulus of elasticity E_T and Young's modulus E_T for steel grade C345-3 are taken equal to 0.92 GPa and 206 GPa, respectively, the remaining values are taken from Table 2.

In numerical modeling of flange joints, it is important to choose the models of the contact parts of the joint [30], [33]. ANSYS allows users to set different models for each contact pair, which are based on different physical and mechanical conditions for the interaction of real objects. In this study, the contact between the flanges in the joint is described using the "Frictional" model, which takes into account the sliding friction force proportional to the magnitude of the normal reaction with a friction coefficient of 0.25. The inner face of the bolt head and the upper face of the flange are connected by the "Bonded" contact, preventing them from moving along the axis of the bolt. In the model of flange joint, solid finite elements with a sampling interval of 10 mm were used. The number of finite elements in the model is 130630. The number of nodes is 224048 (Fig. 4).

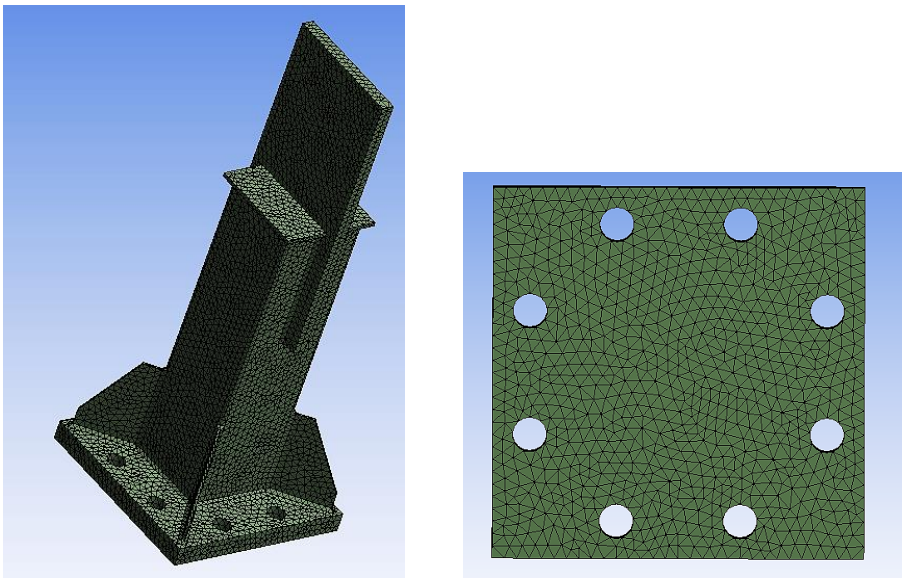

Figure 4. FE model of the joint.

The calculation of the model was carried out in a geometrically and physically nonlinear formulation in the following sequence. Initially, the force of the preliminary tension of the bolts was created, then this state

was fixed, and only after that, the design load equal to 451 kN was applied to the joint. The calculated load was applied with a uniform distribution over the cross-sectional area of the square section profile of the test joint. The restriction on all degrees of freedom as boundary conditions was used on the opposite side of the joint, i.e., the opposite side of the joint was absolutely rigid fixed.

2.4. Metallographic test of bolts

At the third stage of the research, metallographic studies were carried out to assess the effect of non-metallic inclusions on the performance of high-strength bolts. Non-metallic inclusions are a factor in the technological heredity of bolt stock. The typical non-metallic inclusions are oxides and sulfides. At present, non-metallic inclusions are not regulated and are not a defect in assessing the quality of high-strength bolts. A significant fraction of the failure of high-strength bolts is associated with contamination of steel by non-metallic inclusions [34, 35].

The microstructure of the bolt material was studied using an Axio Observer D1.m optical microscope equipped with a Thixomet Pro hardware-software complex for image analysis. The Estimation of the amount and shape of non-metallic inclusions was studied on etched thin sections. To identify the microstructure, the bolt samples were etched in a 4 % solution of nitric acid in ethanol. The hardness was measured by FM-800 microhardness tester with a load of 300 g and by Rockwell hardness tester TP 5014.

3. Results and Discussion

3.1. . Experimental and numerical studies

The results of experimental and numerical studies of the stress-strain state of the analyzed joint are compared in Fig. 5–10. In these figures, the numerator shows the results of the experiment, and the denominator shows the results of numerical calculation.

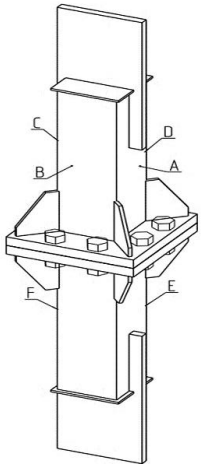

Figure 5. Scheme for marking the surfaces of the sample.

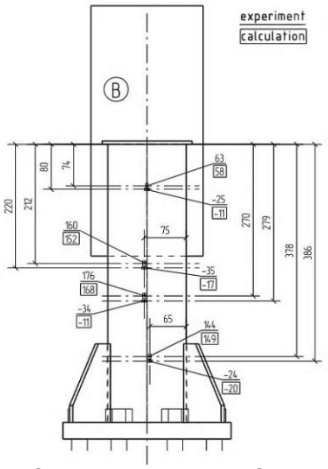

Figure 6. Stress values on surface B, MPa.

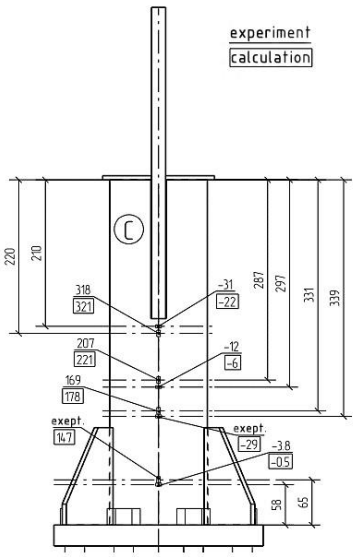

Figure 7. Stress values on surface C, Mpa.

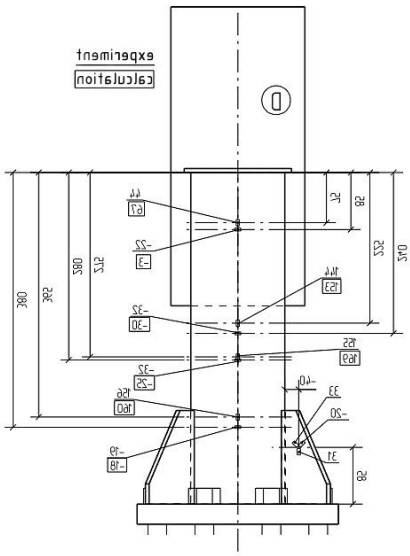

Figure 8. Stress values on surface D, Mpa.

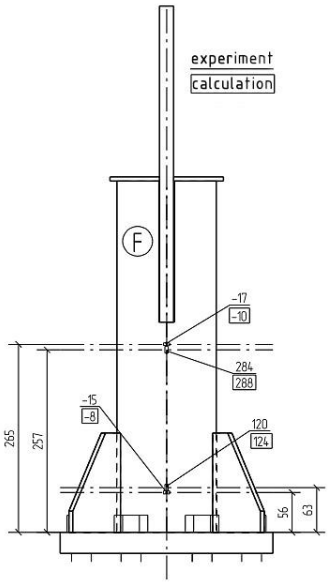

Figure 9. Stress values on surface F, MPa.

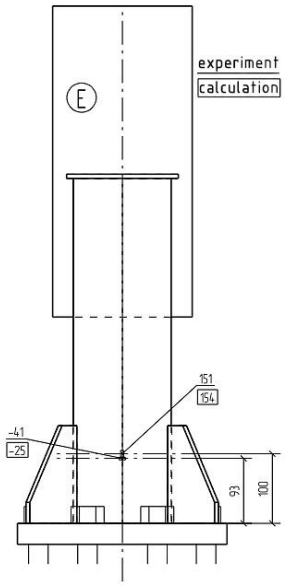

Figure 10. Stress values on surface E, Mpa.

Fig. 7–10 show that tensile forces act in along direction on the part of the chord which is above the stiffening ribs. Those forces create stresses of 160–220 MPa. Compressive forces act in the transverse direction to the chord. The compressive forces create stresses of up to 35 MPa. On the transition area from the free chord to the area with stiffening ribs, the tensile stresses decreased to 120–160 MPa. In this case, the stress created by the compressive forces remains at approximately the same level. Partial unloading of the chord in this section is due to the performance of stiffening ribs, which are in the complex stress state.

It should be noted here that the main stress plates in this case do not coincide with the axes of the strain gauges glued to the stiffening rib. Therefore, the stress values shown in Fig. 7 are somewhat different from the stresses acting in the main stress plates. In particular, the main tensile stresses at this point are 75 MPa, and compressive – 15 MPa. In the other areas, where the rosette of the sensor sticker was used, no significant differences were found.

Maximum stresses in the flange occur in areas under the head and nut of high-strength bolts. The magnitude of these stresses is about 170 MPa (Fig. 11) and is due to the preliminary tension of the bolts. In other parts of the flange, the stress level is much lower and does not exceed 35 MPa. The maximum clearance between the flanges is observed at the installation site of the stiffening ribs, and is 0.2 mm. Under the square section profile, it is slightly smaller and does not exceed 0.15 mm.

The external force applied at one bolt is much less than the force of its preliminary tension. So, for example, when a load of 608 kN is applied to the assembly, only 76 kN falls on one bolt, which is 3.51 times less than the force of its preliminary tension. Due to this fact, any significant changes in the stress-strain state of the bolts were detected neither by experimental nor numerical methods. The clearance between the flanges under the bolts did not appear. The maximum stresses arise in the body of the bolt and is about 600 MPa (Fig. 12).

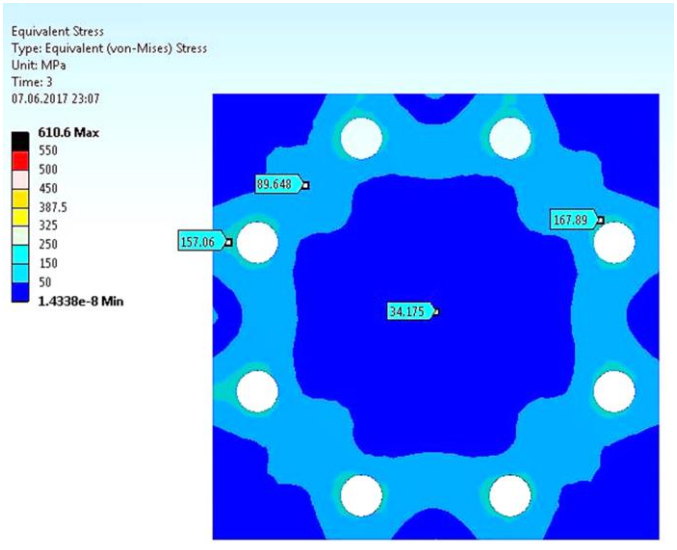

Figure 11. von Mises equivalent stresses on the flange surface [MPa].

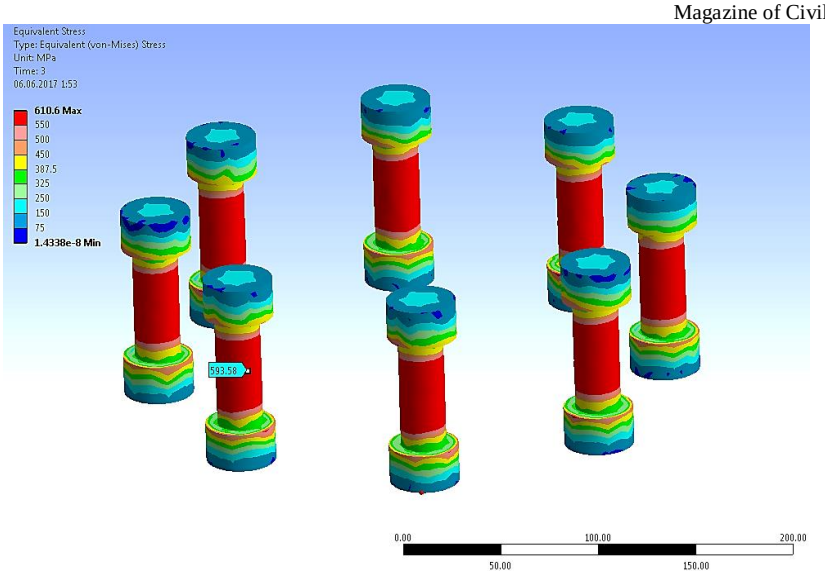

Figure 12. von Mises equivalent stresses in Fasteners [MPa].

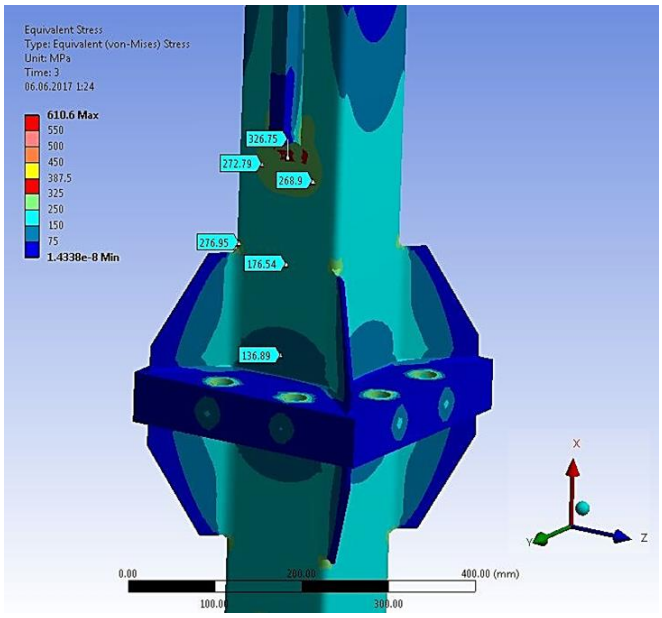

Figure 13. von Mises equivalent stresses in the joint [MPa].

From the analysis of the stress-strain state, it follows that the joint has a large safety margin of strength and that the stress-strain state is non-optimal by the distribution. For example, the most part of flanges and stiffening ribs turned out to be unloaded in comparison with the square section profile. In the chord itself, in the area where the stiffening ribs are adjacent to the profile, in its upper part, the stress is 1.5 times greater than in the rest of the section (Fig. 13).

In most elements, the calculated and experimental values of stresses practically coincide. The maximum difference between them in the most loaded elements does not exceed 10 %. To illustrate the capabilities of the developed finite element model in the studied unit, the thickness of the flanges and the diameter of the bolts was reduced to 20 mm, and the height of the stiffening ribs was increased to 210 mm. From the calculation results it follows that when the design load is applied, the clearance between the flanges under the bolts did not appear, the material of the flange joints behaves elastically.

The increase in the height of the stiffening ribs (L) to the value recommended in [36] with L > 1.5 H, but not less than 200 mm, did not significantly affect the stress-strain state of the horizontal cross-section (Fig. 14). Where H is the cross-sectional depth of the horizontal cross-section.

The decrease in the thickness of the flanges led to an increase in the equivalent stresses in them under the hydraulic fracturing to 62 MPa (Fig. 15), and the clearance between flanges increased to 0.3 mm. The clearance between the flanges under the stiffening ribs has not changed. Thus, it can be stated that the optimized assembly is in a completely operable state and provides material savings and a reduction in the diameter of the bolts.

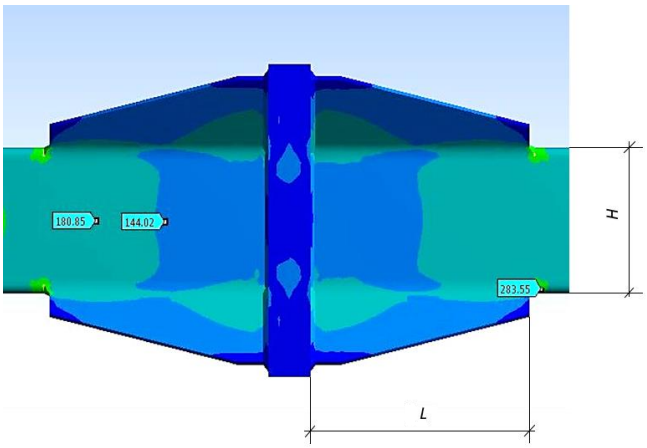

Figure 14. von Mises equivalent stresses in a modified joint [MPa].

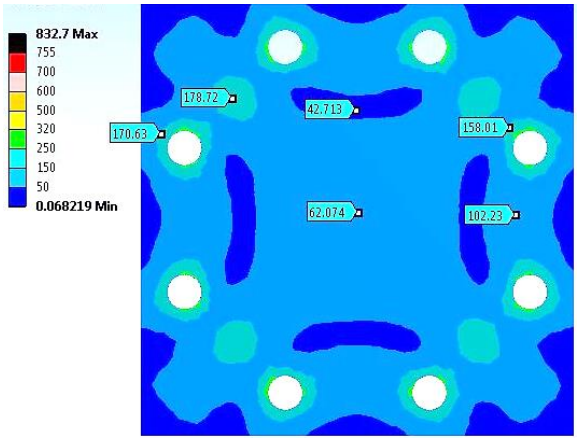

Figure 15. von Mises equivalent stresses on the surface of a modified joint flange [MPa].

3.2. Metallographic studies

The performance of a flange joint depends on the bearing capacity of high-strength bolts. Bolts are critical elements for this type of flange connection. The determination of the bearing capacity of a bolt during its viscous destruction is regulated by current regulatory documents and does not cause difficulties. Problems arise when evaluating the performance of a bolt in the presence of a risk of delayed brittle fracture. Such destruction depends on the saturation of the metal with hydrogen diffusion, the magnitude of tensile stresses, the structure of the steel, and the contamination of its non-metallic inclusions.

Delayed brittle fracture of high-strength bolts is a dangerous type of fracture. It occurs at nominal stresses below the creep limit of the material and is determined by the strength of the grain boundaries in the metal. The state of metal grains depends on several internal factors and varies over time. The main causes of damage are non-metallic inclusions, the size and quantity of which are not regulated by the current regulatory documents for the manufacture of high-strength bolts [34, 35].

Fig. 16 shows the surface crack formed under the head of the M30×160 10.9 bolt. The bolt was made of steel of the Russian grade 40X (Table 3). The crack was detected by visual inspection of the quality of the anti-corrosion coating applied by electrolytic galvanizing.

Table 3. The chemical composition of the steel according to Russian State Standard GOST 4543-2016 "Metal products from structural alloy steel. Technical specifications".

Steel grade	Mass percentage, %							
	C	Mn	Si	Cr	Ni	Cu	S	P
40X	0.36–0.44	0.5–0.8	0.17–0.37	0.8–1.1	≥ 0.30	≥ 0.30	≥ 0.035	≥ 0.035

From the results of metallographic studies, it was found that the microstructure of the bolt material is troostosorbite tempering, which preserves the needle orientation of martensite (Fig. 17). The steel at the crack is not decarburized, the hardness of the bolt meets the requirements of ISO 898-1-2014. The bolt's crack is radial, sinuous, and runs along the grain boundaries. Opened and closed cavity cracks are associated with sulfide inclusions lines. The beginning of the crack lies on the surface of the bolt rod.

The studies of non-etched samples taken from the bolt showed the presence in it of many sulfide inclusions lines. The inclusions identified by Russian State Standard GOST 1778-70 “Steel. Metallographic methods for the determination of non-metallic inclusions” as 2-3 points (Fig. 18, inclusions type 1). Most of these inclusions are located near the crack. In the remaining fields of view of the sample, mainly point oxides and sulfides are present and identified as 2 points (Fig. 18, inclusions type 2).

It can be assumed that crack formation occurred during bolt hardening as a result of the separation of grain-boundary sulfides from the metal matrix under the action of tensile stresses. The final crack opening appeared, most likely, at the stage of electrolytic galvanizing of the bolt due to diffusion of atomic hydrogen into the prefracture zone, which led to a decrease in the cohesive strength of the interphase boundaries between the metal matrix and nonmetallic inclusions.

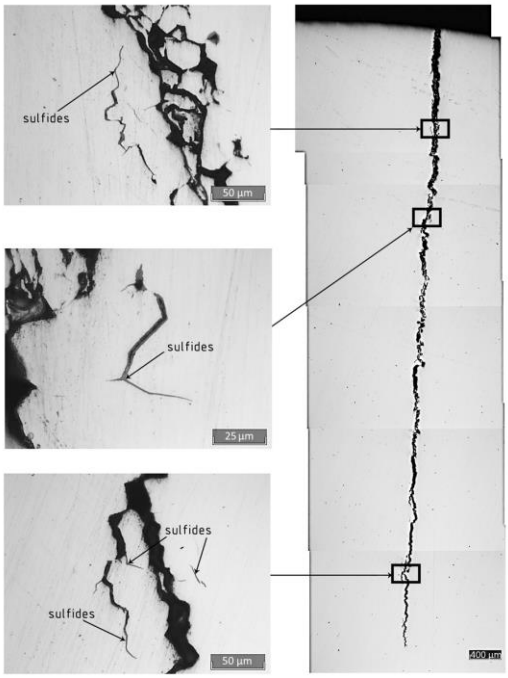

Figure 16. Crack panorama.

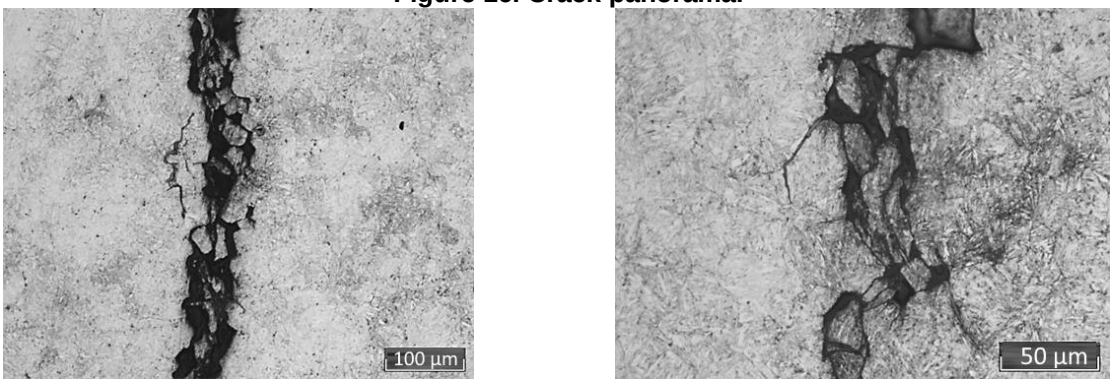

x200 **x500**

Figure 17. The microstructure of the bolt with a crack passing through the grain boundary inclusions.

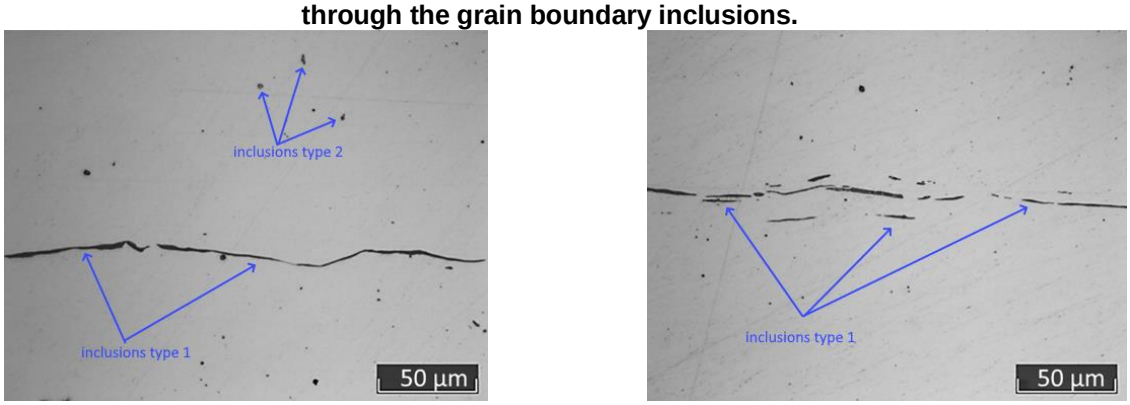

x500 **x500**

Figure 18. Sulfide inclusions lines under the head of a bolt on a longitudinal non-etched section.

Fig. 19 shows a photograph of the fracture surfaces of bolts M30-6gx160 of strength class 10.9 made of steel 40X. The destruction occurred as a result of the separation of the heads in the process of tensioning the bolts with a force less than the designed.

Studies have shown that the main reason for the failure of bolts is the low quality of bolt stock, namely the presence of large precipitates of sulfides along grain boundaries (Fig. 20). Initially, after rolling, the sulfides are oriented in the rolling direction, which coincides with the axis of the bolt shaft. This is not critical for the given scheme of loading the bolt in the seam assembly. However, during stamping of the bolt head, non-metallic inclusions were deformed along with it and, repeating the configuration of the head, extended in the direction perpendicular (with respect to the initial state). When a bolt is tensioned with inclusions oriented perpendicular to the axis of the bolt, grain-boundary sulfides detach from the metal matrix at voltages lower than the design ones (Fig. 21).

Figure 19. Fracture surfaces of severed bolt heads.

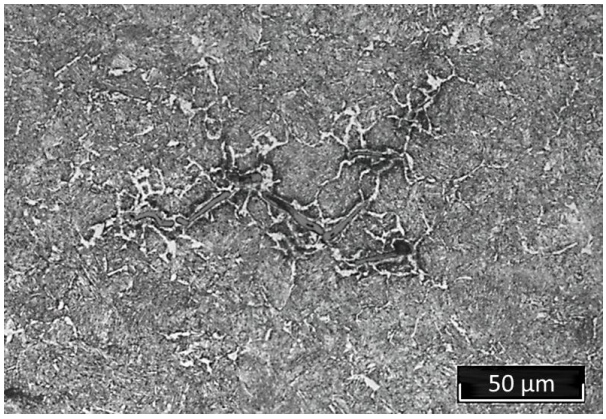

Figure 20. Sulfide precipitation along austenitic grain boundaries.

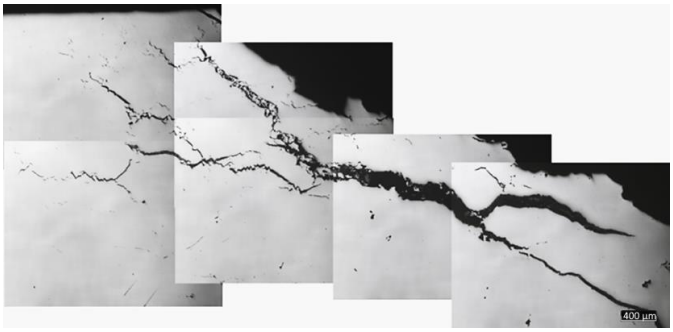

Figure 21. Cavities and cracks oriented perpendicular to the bolt axis under the bolt fracture surface, x50.

The examples of fracture of high-strength bolts discussed above show the need to consider delayed brittle fracture in regulatory documents for the design, manufacture, and assembly of flange joints. The quality of steel for non-metallic inclusions can be ensured by various types of out-of-furnace processing of steel, during which the quantity, size, and shape of non-metallic inclusions are optimized.

For bolts of strength class 10.9 and higher, it is necessary to use microalloyed steel with vanadium, niobium, titanium, and boron. The presence of these elements prevents the growth of austenitic grain during steel hardening, and under certain heat treatment conditions, it allows the formation of a finely dispersed bainitic or bainitic-martensitic structure [9, 37–40]. Such steels have high strength and toughness, better resist delayed brittle fracture, and are not so sensitive to stress concentrators.

Considering the influence of technological heredity on the bearing capacity of high-strength bolts requires more in-depth study and proper reflection in regulatory documents. For example, in the current regulatory documents for the manufacture of bolts, the shape of the hollows of the thread is not regulated and can be either rounded or flat-cut. For high-strength bolts with a strength class of 10.9 and higher, a thread with a rounded hollow profile is preferable, since has a lower concentration of stresses and better resists crack nucleation [9, 41]. The presence of a small and unregulated transition radius at the base of the depression of a plane-cut profile contributes to the formation of microcracks at medium voltages less than design.

Fig. 22 shows macro slices of a flat-section profile of a threaded cavity of a high-strength stud of strength class 10.9 made of steel 30KhGSA in the initial state and after the destruction. The hollow of the thread shown in Fig. 21b was in the third from the place of destruction of the pin, which collapsed after 45 days after its installation.

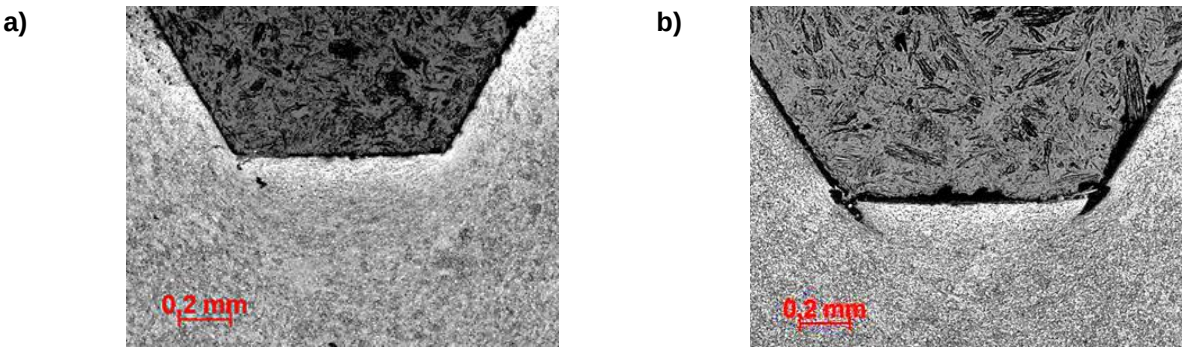

Figure 22. Flat-cut profile of the thread cavity of the stud 2M48-6gx500 10.9 before (a) and after (b) fracture.

4. Conclusions

The flanged joint of the bottom chord of a truss made of a cold-formed closed welded square profile is studied. The joint included rigid flanges with stiffening ribs and high-strength bolts. The stress-strain state of the flange joint was determined by strain gauges testing the full-scale unit. The numerical simulation was performed in ANSYS. Studies of the technological heredity of high-strength bolts were carried out by metallographic and durometric methods.

The results obtained allow to draw the following conclusions:

1. The model solution for a flanged coaxial connection of two square section bent closed welded strip profiles (Fig. 1, 2) provides for the most part a uniform distribution of stresses at the junction due to its spatial rigidity. The presence of stiffening ribs provides the absence of the clearance between the flanges and promotes the joint performance of welded units and high-strength bolts.

2. The disadvantages of this connection include the incomplete loading of flanges and stiffeners in comparison with a square section bent closed welded strip profiles. Stresses in flanges and stiffeners do not exceed 50 MPa. The Field tests of full-size flange joints showed that the destruction of such joints occurs along the body of a section not reinforced with stiffening ribs.

3. The calculation of the flange joint using the developed finite element model indicates that the results of the numerical and experimental studies are sufficient for practical application. The difference between them in the most loaded elements of flange joints does not exceed 10 %.

4. To ensure the bearing capacity of high-strength bolts of strength class 10.9 and higher, which are part of rigid flange joints, it is proposed to introduce regulatory restrictions on the number and size of non-metallic inclusions that affect the delayed brittle fracture of bolts.

5. To improve the performance of high-strength bolts of strength class 10.9 and higher, it is proposed to use steel grades with a bainitic or bainitic-martensitic structure, which are formed by microalloying them with molybdenum, vanadium, niobium, titanium, boron and heat treatment. The strength of such steels reaches 1400–1600 MPa, while their toughness, fracture toughness, as well as resistance to delayed brittle fracture increases.

5. Acknowledgements

The research is partially funded by the Ministry of Science and Higher Education of the Russian Federation as part of World-class Research Center program: Advanced Digital Technologies (contract No. 075-15-2020-934 dated 17.11.2020).

Field tests of flanges were carried out under an agreement with CJSC INSI, Chelyabinsk, Russia. The authors thank master students V.A. Stabel and K.A. Patlusova of the South Ural State University for help in this work.

References

1. Liu, X.-C., Cui, F.-Y., Jiang, Z.-Q., Wang, X.-Q., Xu, L., Shang, Z.-X., Cui, X.-X. Tension–bend–shear capacity of bolted-flange connection for square steel tube column. Engineering Structures. 2019. 201. DOI: 10.1016/j.engstruct.2019.109798
2. Willibald, S. Bolted Connections for Rectangular Hollow Sections under Tensile Loading. Universität Fridericiana zu Karlsruhe, 2003.
3. Yamaguchi, T. Fundamental Study on High Strength Bolted Tensile Joints. Kyoto University, 1996.
4. Leong, S.H., Sulong, N.H.R., Jameel, M. Bolted connections to Tubular columns at ambient and elevated temperatures – A review. Steel and Composite Structures. 2016. 21(2). Pp. 303–321. DOI: 10.12989/scs.2016.21.2.303
5. Liu, X.C., He, X.N., Wang, H.X., Zhang, A.L. Compression-bend-shearing performance of column-to-column bolted-flange connections in prefabricated multi-high-rise steel structures. Engineering Structures. 2018. 160. Pp. 439–460. DOI: 10.1016/j.engstruct.2018.01.026
6. Liu, X.C., Pu, S.H., Zhang, A.L., Zhan, X.X. Performance analysis and design of bolted connections in modularized prefabricated steel structures. Journal of Constructional Steel Research. 2017. 133. Pp. 360–373. DOI: 10.1016/j.jcsr.2017.02.025
7. Hoang, V.L., Jaspart, J.-P., Demonceau, J.-F. Behaviour of bolted flange joints in tubular structures under monotonic, repeated and fatigue loadings I: Experimental tests. Journal of Constructional Steel Research. 2013. 85. Pp. 1–11. DOI: 10.1016/j.jcsr.2013.02.011
8. Álvarez, J.A., Lacalle, R., Arroyo, B., Cicero, S., Gutiérrez-Solana, F. Failure analysis of high strength galvanized bolts used in steel towers. Metals. 2016. 6(7). DOI: 10.3390/met6070163
9. Tingaev, A.K., Gubaydulin, R.G., Shaburova, N.A. Causes of Failure of High-Tensile Stud Bolts Used for Joining Metal Parts of Tower Crane. IOP Conference Series: Materials Science and Engineering. 2017. 262(1). DOI: 10.1088/1757-899X/262/1/012058
10. Willibald, S., Packer, J.A., Puthli, R.S. Experimental study of bolted HSS flange-plate connections in axial tension. Journal of Structural Engineering. 2002. 128(3). Pp. 328–336. DOI: 10.1061/(ASCE)0733-9445(2002)128:3(328)
11. Kato, B., Mukai, A. Bolted tension flanges joining square hollow section members. Journal of Constructional Steel Research. 1985. 5(3). Pp. 163–177. DOI: 10.1016/0143-974X(85)90001-X
12. EN 1993-1-8: Eurocode 3: Design of steel structures – Part 1-8: Design of joints.
13. Standard Specifications for Steel and Composite Structures. English version Tokyo, 2009.
14. Wang, X., Wang, Y., An, Q. Moment Resistance and Stiffness of an Assembled Beam-Column Joint with High-Strength Bolt and External Diaphragm | 装配式梁柱外环板高强螺栓连接节点抗弯承载力及节点刚度研究. Tianjin Daxue Xuebao (Ziran Kexue yu Gongcheng Jishu Ban)/Journal of Tianjin University Science and Technology. 2019. 52. Pp. 75–82. DOI: 10.11784/tdxbz201904086
15. Liu, X., He, X., Zhang, A., Wang, H., Zhan, X., Xu, L. Bearing performance of bolted-flange connection of square steel tubular column under tension-bend-shearing combination | 拉-弯-剪组合作用下法兰连接方钢管柱受力性能研究. Jianzhu Jiegou Xuebao/Journal of Building Structures. 2018. 39(6). Pp. 69–80. DOI: 10.14006/j.jzjgxb.2018.06.008
16. Nadolski, V. Calculation and Construction of the Flange Connection of Rectangular Elements Subjected to the Axial Tension. Vestnik of PSU. Part F. Constructions. Applied Sciences. 2018. (8). Pp. 121–130.
17. Ismail, R.E.S., Fahmy, A.S., Khalifa, A.M., Mohamed, Y.M. Numerical study on ultimate behaviour of bolted end-plate steel connections. Latin American Journal of Solids and Structures. 2016. 13(1). Pp. 1–22. DOI: 10.1590/1679-78251579
18. Tarleton, E. Incorporating hydrogen in mesoscale models. Computational Materials Science. 2019. 163. Pp. 282–289. DOI: 10.1016/j.commatsci.2019.03.020
19. Wang, Y., Jia, S., Chai, W. Experimental Study and Numerical Analysis of T-Stub Connections with Single Direction High Strength Bolts | 单边高强螺栓 T 型件连接节点试验研究及数值模拟. Tianjin Daxue Xuebao (Ziran Kexue yu Gongcheng Jishu Ban)/Journal of Tianjin University Science and Technology. 2018. 51. Pp. 78–85. DOI: 10.11784/tdxbz201804057
20. Brahimi, S.V., Yue, S., Sriraman, K.R. Alloy and composition dependence of hydrogen embrittlement susceptibility in high-strength steel fasteners. Philosophical Transactions of the Royal Society A: Mathematical, Physical and Engineering Sciences. 2017. 375(2098). DOI: 10.1098/rsta.2016.0407
21. Akiyama, E. Evaluation of delayed fracture property of high strength bolt steels. ISIJ International. 2012. 52(2). Pp. 307–315. DOI: 10.2355/isijinternational.52.307
22. Hagihara, Y. Evaluation of delayed fracture characteristics of high-strength bolt steels by CSRT. ISIJ International. 2012. 52(2). Pp. 292–297. DOI: 10.2355/isijinternational.52.292
23. Major, I., Major, M., Kuliński, K. The influence of high-strength bolts stiffening on flange connection behaviour. Engineering Transactions. 2019. 67(2). Pp. 199–211. DOI: 10.24423/EngTrans.1006.20190405
24. Bao, W., Jiang, J., Yu, Z., Zhou, X. Mechanical behavior of high-strength bolts in T-stubs based on moment distribution. Engineering Structures. 2019. 196. Pp. 109334. DOI: 10.1016/j.engstruct.2019.109334
25. Tuan, L.A. Behavior of ring flange – Bolts joint under complex bearing forces. International Journal of Engineering and Advanced Technology. 2019. 9(1). Pp. 7352–7358. DOI: 10.35940/ijeat.A2224.109119
26. Shafray, K., Shafray, S. Work flange connections of structural elements of an open profile on high-strength bolts. Journal of Physics: Conference Series. 1425(1) 2020. Pp. 012072.
27. ISO 16573:2015, Steel — Measurement method for the evaluation of hydrogen embrittlement resistance of high strength steels.
28. Popov, A., Babak, S. Effect of cutting modes and tool wear on the microhardness of the surface layer after face milling of structural and stainless steels. Manufacturing Technology. 2018. 18(6). Pp. 1011–1014. DOI: 10.21062/ujep/216.2018/a/1213-2489/mt/18/6/1011
29. Couchaux, M., Hjiaj, M., Ryan, I., Bureau, A. Effect of contact on the elastic behaviour of tensile bolted connections. Journal of Constructional Steel Research. 2017. 133. Pp. 459–474. DOI: 10.1016/j.jcsr.2016.10.012
30. Couchaux, M., Hjiaj, M., Ryan, I., Bureau, A. Tensile resistances of bolted circular flange connections. Engineering Structures. 2018. 171. Pp. 817–841. DOI: 10.1016/j.engstruct.2018.04.004

31. Semenov, A.A., Malyarenko, A.A., Porivaev, I.A., Safiullin, M.N. Stress-strain behavior investigation of friction grip bolts in flange joints of trusses. Magazine of Civil Engineering. 2014. 49(5). Pp. 54–62, 131–132. DOI: 10.5862/MCE.49.6
32. Priadko, I.N., Mushchanov, V.P., Bartolo, H., Vatin, N.I., Rudnieva, I.N. Improved numerical methods in reliability analysis of suspension roof joints. Magazine of Civil Engineering. 2016. 65(5). Pp. 27–41. DOI: 10.5862/MCE.65.3
33. Kim, J., Yoon, J.-C., Kang, B.-S. Finite element analysis and modeling of structure with bolted joints. Applied Mathematical Modelling. 2007. 31(5). Pp. 895–911. DOI: 10.1016/j.apm.2006.03.020
34. Álvarez, J.A., Lacalle, R., Arroyo, B., Cicero, S., Gutiérrez-Solana, F. Failure analysis of high strength galvanized bolts used in steel towers. Metals. 2016. 6(7). Pp. 163. DOI: 10.3390/met6070163
35. Brahimi, S.V., Yue, S., Sriraman, K.R. Alloy and composition dependence of hydrogen embrittlement susceptibility in high-strength steel fasteners. Philosophical Transactions of the Royal Society A: Mathematical, Physical and Engineering Sciences. 2017. 375(2098). Pp. 20160407. DOI: 10.1098/rsta.2016.0407
36. Kalenov, V.V. Eksperimentalno-teoreticheskoe issledovanie i sovershenstvovanie metodov proektirovaniia boltovykh montazhnykh soedinenii stalnykh stroitelnykh konstruktcii [Experimental and theoretical research and improvement of design methods for bolted mounting joint. Melnikov Central Research and Design Institute of Steel Structures, Moskow, Russia, 1995.
37. Ooi, S.W., Ramjaun, T.I., Hulme-Smith, C., Morana, R., Drakopoulos, M., Bhadeshia, H.K.D.H. Designing steel to resist hydrogen embrittlement Part 2–precipitate characterisation. Materials Science and Technology (United Kingdom). 2018. 34(14). Pp. 1747–1758. DOI: 10.1080/02670836.2018.1496536
38. Ramjaun, T.I., Ooi, S.W., Morana, R., Bhadeshia, H.K.D.H. Designing steel to resist hydrogen embrittlement: Part 1–trapping capacity. Materials Science and Technology (United Kingdom). 2018. 34(14). Pp. 1737–1746. DOI: 10.1080/02670836.2018.1475919
39. Das, T., Sriraman, K.R., Brahimi, S.V., Song, J., Yue, S. A study on the susceptibility of high strength tempered martensite steels to hydrogen embrittlement (HE). ICF 2017 – 14th International Conference on Fracture. 22017. Pp. 974–976.
40. Das, T., Rajagopalan, S.K., Brahimi, S.V., Wang, X., Yue, S. A study on the susceptibility of high strength tempered martensite steels to hydrogen embrittlement (HE) based on incremental step load (ISL) testing methodology. Materials Science and Engineering A. 2018. 716. Pp. 189–207. DOI: 10.1016/j.msea.2018.01.032
41. Eder, M.A., Haselbach, P.U., Mishin, O.V. Effects of Coatings on the High-Cycle Fatigue Life of Threaded Steel Samples. Journal of Materials Engineering and Performance. 2018. 27(6). Pp. 3184–3198. DOI: 10.1007/s11665-018-3399-2

Contacts:

Nikolai Vatin, vatin@mail.ru
Rafkat Gubaydulin, gubaidulinrg@susu.ru
Aleksandr Tingaev, tingaevak@susu.ru